Ecotoxicology and Environmental Safety 220 (2021) 112402

Contents lists available at ScienceDirect

Ecotoxicology and Environmental Safety

journal homepage: www.elsevier.com/locate/ecoenv

Protective effects of cerium oxide nanoparticles in grapevine (*Vitis vinifera* L.) cv. Flame Seedless under salt stress conditions

Gholamreza Gohari [a,*], Elnaz Zareei [b], Havzhin Rostami [a], Sima Panahirad [b], Muhittin Kulak [c], Habib Farhadi [a], Mojtaba Amini [d,e], Maria del Carmen Martinez-Ballesta [f], Vasileios Fotopoulos [g]

[a] Department of Horticultural Sciences, Faculty of Agriculture, University of Maragheh, Maragheh, Iran
[b] Department of Horticultural Sciences, Faculty of Agriculture, University of Tabriz, Tabriz, Iran
[c] Department of Herbal and Animal Production, Vocational School of Technical Sciences, Igdir University, Turkey
[d] Department of Chemistry, Faculty of Sciences, University of Maragheh, Maragheh, Iran
[e] Department of Inorganic Chemistry, Faculty of Chemistry, University of Tabriz, Tabriz, Iran
[f] Department of Agronomy Engineering, Universidad Politécnica de Cartagena, Paseo Alfonso, Cartagena, Spain
[g] Department of Agricultural Sciences, Biotechnology and Food Science, Cyprus University of Technology, Limassol, Cyprus

ARTICLE INFO

Edited by Professor Bing Yan

Keywords:
Abiotic stress
Cerium oxide
Nanotechnology
Salt stress
Nutrient elements

ABSTRACT

High levels of soil salinity can cause substantial decline in growth and productivity of crops worldwide, thus representing a major threat to global agriculture. In recent years, engineered nanoparticles (NPs) have been deemed as a promising alternative in combating abiotic stress factors, such as salinity. In this context, the present study was designed to explore the potential of cerium oxide nanoparticles (CeO_2NPs) in alleviating salt stress in grapevine (*Vitis vinifera* L. cv. Flame Seedless) cuttings. Specifically, the interaction between CeO_2 NPs (25, 50 and 100 mg L^{-1}) and salinity (25 and 75 mM NaCl) was evaluated by assaying an array of agronomic, physiological, analytical and biochemical parameters. Treatments with CeO_2 NPs, in general, alleviated the adverse impacts of salt stress (75 mM NaCl) significantly improving relevant agronomic traits of grapevine. CeO_2 NPs significantly ameliorated chlorophyll damage under high levels of salinity. Furthermore, the presence of CeO_2 NPs attenuated salinity-induced damages in grapevine as indicated by lower levels of proline, MDA and EL; however, H_2O_2 content was not ameliorated by the presence of CeO_2 NPs under salt stress. Additionally, salinity caused substantial increases in enzymatic activities of GP, APX and SOD, compared with control plants. Similar to stress conditions, all concentrations of CeO_2 NPs triggered APX activity, while the highest concentration of CeO_2 NPs significantly increased GP activity. However, CeO_2 NPs did not significantly modify SOD activity. Considering mineral nutrient profile, salinity increased Na and Cl content as well as Na/K ratio, while it decreased K, P and Ca contents. Nevertheless, the presence of CeO_2 NPs did not lead to significant alterations in Na, K and P content of salt-stressed plants. Taken together, current findings suggest that CeO_2 NPs could be employed as promising salt-stress alleviating agents in grapevine.

1. Introduction

Salinity, representing a major abiotic stress factor, causes substantial alterations in osmotic potential and cellular water content, which in turn result in reduction of quality and quantity of the yield of horticultural crops (Fraga et al., 2012; Yuanchun et al., 2015). Concerning potential consequences of high salinity on vineyard development and productivity, leaf burns or death and subsequent significant yield loss have been observed, in accordance with reductions in photosynthetic and leaf expansion rates (Fisarakis et al., 2001; Munns, 2002; Walker et al., 2002). Physiologically, plant growth is affected by salinity in a variety of ways. The first phase of the growth response under salt stress is affected by similar symptoms as those observed in water-stressed plants due to osmotic perturbances (Munns et al., 1995; Munns, 2002). Salt stress and water deficit result in slight inhibition of growth and degradation of photosynthetic pigments in the leaf (Kumar et al., 2017; Kozminska et al., 2018). A large amount of leaf injury and even plant death in some cases emerges when salts accumulate over time in older leaves (Munns, 2002; Munns et al., 1995). High salinity is followed by accumulation of specific osmolytes in the leaf, as well as oxidative stress induction

* Corresponding author.
E-mail address: gohari.gh@maragheh.ac.ir (G. Gohari).

https://doi.org/10.1016/j.ecoenv.2021.112402
Received 22 February 2021; Received in revised form 5 May 2021; Accepted 31 May 2021
Available online 2 June 2021

(manifested as accumulation of malondialdehyde (MDA), induction of ascorbate peroxidase (APX) and glutathione reductase (GR) activity, and increase in total phenolic compound levels and antioxidant flavonoids). High levels of salinity are also known to induce Na^+ and Cl^- accumulation in leaves and roots as well as superoxide dismutase (SOD) and catalase (CAT) activities (AbdElgawad et al., 2016; Kumar et al., 2017).

Wide applications of engineered nanoparticles (NPs) have been carried out in the agricultural sector (Sharon et al., 2010; Yuhui et al., 2015; Ioannou et al., 2020). Relevant biochemical findings showed that such particles significantly alter photosynthetic processes, oxidative stress, gene expression, and antioxidant enzymatic activities in plants. It has been reported that nanoparticles such as CeO_2 NPs improve plant tolerance to abiotic stress, largely by enhancing the capacity of their antioxidant system (Sharma et al., 2019; Gohari et al., 2020a, 2020b; Mohammadi et al., 2021). Cerium (Ce) is a rare earth metal and can exist in the Ce^{3+} (cerous) and Ce^{4+} (ceric) oxidation states acting as oxygen buffer. Potential effects of CeO_2 NPs on plant health, either positive or negative, depend on plant growth conditions, plant species, and exposure concentration and duration (Wang et al., 2012; Zhao et al., 2014; Ma et al., 2016a, 2016b). However, the mechanisms of CeO_2 NP impacts at different concentrations are not fully understood, likely due to the duel valance states of Ce on the nanoparticle surface. This makes CeO_2 NPs perform either as an antioxidant (Wang et al., 2012) or pro-oxidant under different conditions (Ma et al., 2016a, 2016b). Given the likelihood of NP accumulation in saline agricultural soils, some studies have emerged that examine the synergistic effects of these two factors (NPs and salinity) in plants. Zayed et al. (2017) reported the promoted seed germination and radical length of bean plants under salt stress treated with different concentrations of nano-chitosan. Moringa plants sprayed with Hoagland's solutions containing ZnO NPs and Fe_3O_4 NPs displayed enhanced growth parameters under both normal and saline conditions compared with controls (Soliman et al., 2015). Authors also stated a significant increase of some essential macro- and micro-elements, total chlorophyll, carotenoids, proline and carbohydrates in plant tissues and a significant decrease in Na^+ and Cl^- content.

In addition, significant enhancement of spinach plant growth through further activation of the photosynthesis process following TiO_2 NP treatment has been reported (Zheng et al., 2005). Likewise, TiO_2 NP supplementation led to the significant increase in enzymatic antioxidant activities and soluble sugars, amino acids, and proline content in salt-affected broad bean plants compared with plants subjected to salinity alone (AbdelLatef et al., 2018). Considering the extent of CeO_2 NPs effects in plants and their unique surface redox chemistry, it is intriguing to investigate the responses of grapevines as relatively sensitive plants to salinity stress exposed to the synthesized CeO_2 NPs.

2. Material and methods

2.1. Preparation and characterization of CeO_2 nanoparticles

CeO_2 nanoparticles were synthesized according to our previously reported procedure (Amini et al., 2016). An aqueous solution (10 mL) of $Ce(NO_3)_3$. $6H_2O$ (1.0 g) was basified with a NaOH solution (1.0 M), and a white precipitate of $Ce(OH)_4$ was obtained. The solid of $Ce(OH)_4$ was filtered and, after washing several times with water, was dried under air. 1 g of urea (as a fuel) was mixed and pulverized with $Ce(OH)_4$ and, the residual solid was calcinated after grinding at 400 °C for 5 h. The synthetic CeO_2 NPs were characterized by XRD, EDAX and SEM analysis.

2.2. Plant material and experimental design

This study was carried out at the research greenhouse of the Faculty of Agriculture, University of Maragheh, Maragheh, Iran (longitude 46°16' E, latitude 37°23' N, altitude 1485 m), using a completely randomized design (CRD) as a factorial experiment with three replications. Four-year-old cuttings of grapevine cv. Flame Seedless were purchased from West Azerbaijan Agriculture and Natural Resources Research Center, ARREO, Urmia, Iran and were planted in 7 L pots containing a mixture of coco peat and medium grain perlite in a ratio of 3:1. Plants were irrigated daily with quarter-strength Hoagland solution for a month until at least eight true leaves emerged (each pot contained a cutting). After one month, salinity stress (0, 25 and 75 mM NaCl) was imposed daily (in combination with half-strength Hoagland solution) and continued for 2 months. Nanomaterial treatments including four levels of CeO_2 NPs (0, 25, 50 and 100 mg L^{-1}) were applied 30 days after imposing salinity stress by spraying leaves four times with 24 h intervals. Tween® 20% was used for better fixation and penetrability of CeO_2 NP treatments to leaf surfaces. Control plants were daily irrigated with half-strength Hoagland solution until harvest and foliar-sprayed with distilled water (without salinity and CeO_2 NPs). All measured parameters were analysed four weeks after the CeO_2 NP treatment applications, while salinity stress continued until the end of the experiment. Three technical replicates were used for each parameter corresponding to each experimental group. The treatment name was abbreviated in following from: NaCl (**S0**: 0 mM; **S1**: 25 mM, **S2**: 75 mM), CeO_2 NPs (**NP0**: 0 mg L^{-1}; **NP1**: 25 mg L^{-1}; **NP2**: 50 mg L^{-1}, and **NP3**: 100 mg L^{-1}) (Table 1).

2.3. Growth parameters and relative water content

The plant height and leaf number were measured at the harvest stage. Leaf area (cm^2) was measured using a leaf area meter (LI-3100; LI Core, USA). Relative water content (RWC) was measured according to Ritchie et al. (1990).

2.4. Chlorophyll fluorescence and SPAD

Leaf chlorophyll fluorescence measurements were carried out using a dual-pam-100 chlorophyll fluorometer (Heinz Walz, Effeltrich, Germany) based on Maxwell and Johnson (2000). Leaves at the third or fourth nodes of the plant were acclimated to the dark at least 20 min before measurements and $^{Fv}/_{Fo}$, $^{Fv}/_{Fm}$, Y (NO) and Y (II) traits were calculated from these data. The values of SPAD (leaf chlorophyll concentration) were quantified following the method described by Ling et al. (2011) using a SPAD-meter (502 Plus Chlorophyll Meter, Minolta Camera Co., Osaka, Japan).

2.5. Photosynthetic pigment content

Chlorophyll extraction (chlorophyll *a*, *b* and carotenoid contents) and quantification was carried out using young and fully expended leaves at third or fourth nodes of plants according to Sharma et al. (2012). Absorbances of the samples were read at 664 and 647 nm using a UV-Vis spectrophotometer (UV-1800 Shimadzu, Japan).

Table 1
Experimental design of the study.

Acronym	Nanoparticles treatment (mg L^{-1})	Salinity level (mM)
S0NP0	0	0
S1NP0	0	25
S2NP0	0	75
S0NP1	25	0
S1NP1	25	25
S2NP1	25	75
S0NP2	50	0
S1NP2	50	25
S2NP2	50	75
S0NP3	100	0
S1NP3	100	25
S2NP3	100	75

2.6. Electrolyte leakage (EL)

The initial electrical conductivity (EC1) of fully expanded leaves at third or fourth nodes of plants (at ambient temperate for24h) was measured using a conductivity meter (Hanna, HI98192, Hanna Instruments, Inc., Woonsocket, RI, USA). The final electrical conductivity (EC2) was measured in the incubated samples in a water bath at 95 °C for 20 min. The percentage of electrolyte leakage (EL) was calculated as follows (Nayyar, 2003).

$$EL\ (\%) = (EC1/EC2) \times 100$$

2.7. Mineral content

Leaf samples (0.1 g) were oven-dried at 60 °C in a forced air oven (DHG-9023A, Nanjing, China) for 16 h and then ground in a Willey mill and the powered samples were stored for further analyses. Total contents of Na^+ and K^+ (mg g^{-1} DW) were determined by flame photometer (M410 Sherwood, UK) as described by Ghosh (1993). Chloride was measured with Ion-Analyzer using a chloride electrode (ISM146-Cl, Los Angeles, USA) and P concentration in digested samples was estimated after coloring with molybdate-vanadate using spectrophotometer (UV-1800 Shimadzu, Japan) (Ryan et al., 2001).

2.8. Malondialdehyde (MDA) and H_2O_2 quantification

Malondialdehyde (MDA) and H_2O_2 content of leaf TCA extracts were determined as previously described by Stewart and Bewley (1980) and Sinha et al. (2005), respectively. For MDA content, fresh leaf samples were extracted using acetic acid and the extracts were then mixed with thiobarbituric acid in trichloroacetic acid (TCA; 1:11 v/v) for 30 min at 96 °C. The mixture was incubated at 0 °C for 5 min and centrifuged at 10,000 g for 5 min. The absorbance was read at 532 and 600 nm by the spectrophotometer (UV-1800 Shimadzu, Japan). In order to quantify the content of MDA (nM g^{-1} FW), the following equation was applied.

$$MDA\ (nmol\ g^{-1}\ FW) = [(A352\text{-}A600) * V * 1000/\ \varepsilon] * W$$

Where: ε, specific extinction coefficient (155 mM^{-1} cm^{-1}); V, volume of crushing medium; W; leaf fresh weight; A 600, absorbance at 600 nm; A 532, absorbance at 532 nm (Stewart and Bewley, 1980).

For H_2O_2 quantification, fresh leaf samples (0.1 g) were homogenized using trichloroacetic acid (0.1% w/v) (at 0 °C). Homogenization was followed by the addition of potassium phosphate buffer (pH 6.8, 10 mM) and potassium iodide (1 M) to the supernatants. Then, the absorbance was read at 390 nm (UV-1800 Shimadzu, Japan). Different H_2O_2concentrations were used to obtain the standard calibration curve for quantification of H_2O_2content (μM g^{-1} FW; Sinha et al. 2005).

2.9. Proline content

The content of proline (μM g^{-1} FW) was detected using ninhydrin method as described by Bates et al. (1973). Briefly, fresh leaf samples (0.5 g) were subjected to extraction with aqueous sulfosalicylic acid (3%) in ice bath and subsequently the extracted tissues were mixed with solution of proline, ninhydrin and glacial acetic acid (1:1:1). Then, the mixture was incubated for 1 h at 100 °C and placed in an ice bath. Toluene was added and mixed strongly (20 s). The absorbances of the samples were read at 520 nm using a UV-Vis spectrophotometer (UV-1800 Shimadzu, Japan). Different concentration of L-proline was used for standard curve and final calculation of proline values.

2.10. Antioxidant enzymatic activities

First, fresh leaf samples (0.5 g) were homogenized with potassium phosphate buffer (pH6.8, 100 mM) including 1% PVP and EDTA (4 mM) by using magnetic stirrer (10 min) and then homogenate was centrifuged (6000 g, 20 min). The supernatants were used for measuring the total soluble proteins (Bradford, 1976), the activities of ascorbate peroxidase (APX) (Nakano and Asada, 1981), guaiacol peroxidase (GP) (Tang and Newton, 2005) and superoxide dismutase (SOD) enzymes (Flohe and Günzler, 1984) using a UV-Vis spectrophotometer. Results were expressed as U g^{-1} FW. All relevant experiments were performed at 4 °C.

2.11. Statistical analysis

Two-way ANOVA analysis was applied to the data. The variances were related to the main treatments (nanoparticles and salinity) and to their interactions. The means were separated by using Duncan's multiple range test at 5% probability level ($p < 0.05$) (SPSS V.22). Moreover, a principal component analysis (PCA) was performed in order to discriminate the treatments of nanoparticles and salinity on the basis of agronomic traits, physiological attributes, enzymatic activities and status of elemental uptake (XLSTAT). Furthermore, a heat map corresponding to the findings along with the treatments were constructed for visualizing and relating the dependent and independent variables (ClustVis).

3. Results

3.1. CeO_2 nanoparticle characterization

X-ray diffraction (XRD) pattern of CeO_2 NPs was recorded to determine the structure and phase formation of the prepared particles (Fig. 1a). The diffraction patterns of the sample showed the characteristic peaks of the cubic fluorite structured CeO_2 crystal with no peaks of impurity. Energy-dispersive X-ray spectroscopy (EDXS) confirmed the presence of Ce and O in the prepared sample (Fig. 1b). Information about the surface of CeO_2 NPs was obtained by scanning electron microscopy (SEM) as presented in Fig. 1c. The SEM image revealed that particles are formed with diameters in the range of nanometers.

3.2. Biomass, relative water content and growth parameters

As shown in Table S1, salinity and CeO_2 NPs had a substantial effect on FW and DW of leaves (Fig. 2a, b). However, interaction between salinity and CeO_2 NPs did not exhibit significant effects on either FW or DW of the leaf samples. The FW and DW were decreased as salinity concentration increased (0–75 mM). By contrast, FW and DW were enhanced by increasing concentrations of CeO_2 NPs (0–100 mg L^{-1}). The maximum and minimum values of RWC were recorded at treatments of S0NP0 (76.35%) and S2NP1 (66.03%), respectively. Salinity and NP treatments, as well as their interactions, were found to have significant effects in leaf area, leaf number and plant height (Table 2). Accordingly, the highest leaf area was observed when plants were exposed to S0NP2 and S0NP3in leaf areas compared with control. However, lowest leaf area values were recorded in grapevines treated with S2NP0. Furthermore, results showed that treatment of plants with CeO_2NPs (S0NP3 followed by S0NP2) led to a 25% increase in leaf number in comparison with control samples. The lowest number of leaves was obtained in S2NP0-treated plants. In the case of plant height, the highest and lowest heights were observed in plants exposed to S0NP2 and S2NP0, respectively. Compared with control group (S0NP0), plant height increased by up to 12.5% with CeO_2 NP treatment (S0NP2).

3.3. Photosynthetic pigments

Photosynthetic pigments (Chl *a* and *b*), with the exception of carotenoids, were affected by interaction of salinity with CeO_2 NPs (Table S1). The highest content of Chl *a* was detected in S0NP2

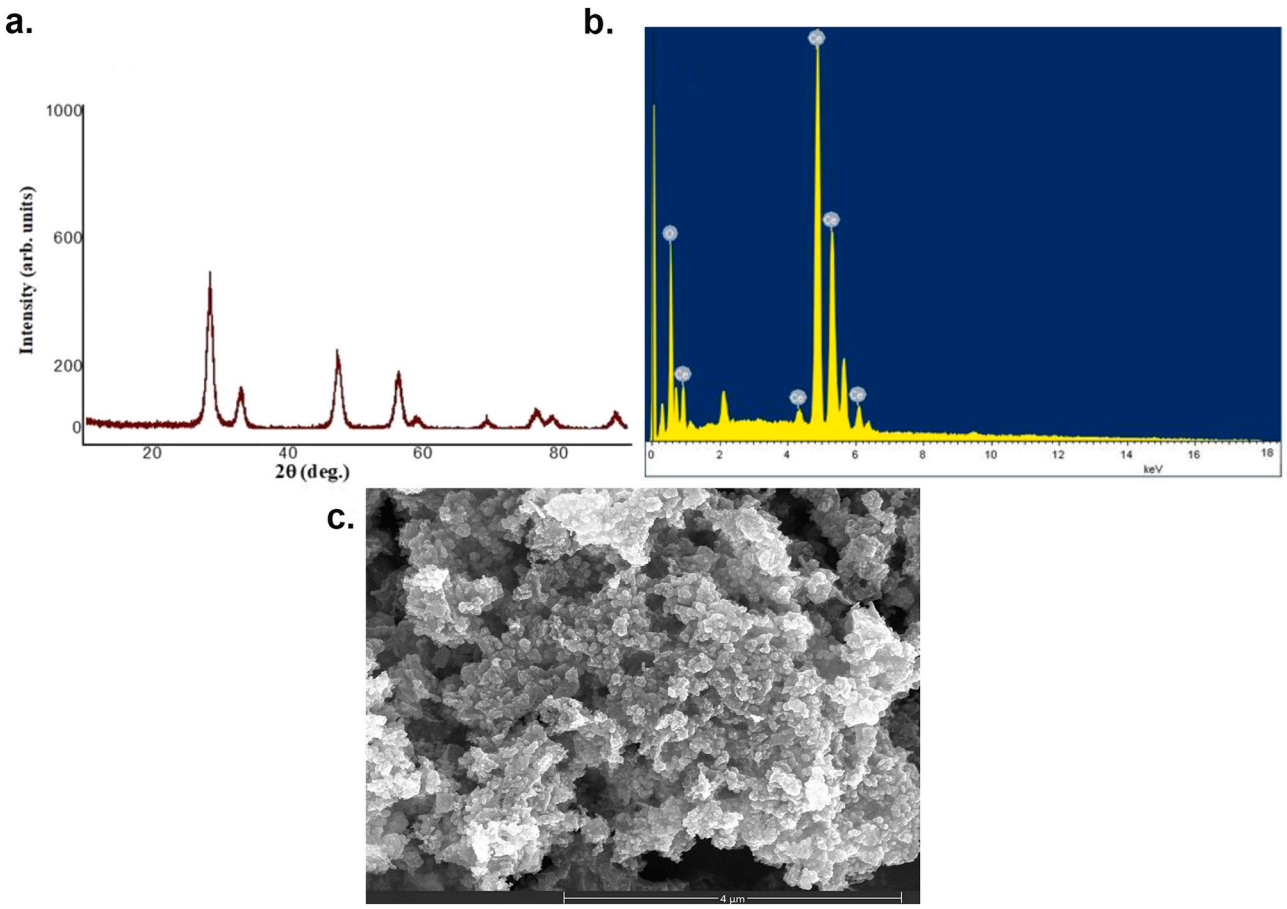

Fig. 1. XRD pattern (a); EDXS analysis (b) and SEM image (c) of the prepared CeO_2 nanoparticles.

treatment (6.22 mg g^{-1} FW), while the lowest Chl *a* was observed in S2NP1 treatment (2.4 mg g^{-1} FW). The highest and lowest Chl *b* contents were detected in the S0NP2 (2.5 mg g^{-1} FW) and S2NP3 (0.51 mg g^{-1} FW) treatments, respectively (Table 2). There was no significant difference in the carotenoid content of plants treated with both salinity and CeO_2 NPs (Fig. 2c).

3.4. Chlorophyll fluorescence and SPAD

Salinity caused a significant reduction in $^{Fv}/_{Fm}$ ($p = 0.0001$). Compared with control samples, salinity decreased $^{Fv}/_{Fm}$ by about 14.3%, whereas it increased in plants treated with CeO_2 NPs ($p = 0.001$). A 3.6-fold increase in values of $^{Fv}/_{Fm}$ was observed in plants treated with 50 mg $L^{-1}CeO_2$NPs in comparison with controls (Fig. 2d). However, the interaction of NP treatments with salinity was not significant ($p = 0.987$). In the case of SPAD values, a significant decrease (~9%) was seen following stress imposition with 75 mM NaCl compared with controls ($p = 0.0001$) (Fig. 3a). Similar to F_v/F_m, a strong increase in SPAD values was recorded in plants treated with CeO_2 NPs ($p = 0.0001$). SPAD increased by 18.9% in plants treated with 50 mg L^{-1} CeO_2 NPs compared with control plants. The interaction of NP treatments with salinity was not significant concerning $^{Fv}/_{Fm}$, values ($p = 0.112$). Based on the results, no significant difference was observed in the Y (NO) and Y (II) traits in plants exposed to salinity and CeO_2 NP treatments (Fig. 3b, c).

3.5. Electrolyte leakage (EL) and Relative Water Content (RWC)

As it is well-known for higher plants, salinity causes significant membrane damage at high concentrations. A clear damage of cell membrane, determined as EL, was noted with increasing salinity levels, but the increases in EL due to salinity were ameliorated by NP treatments. The EL values of NP-treated plants were significantly lower than those of both control and salt-stressed plants. Thus, plants exposed to S2NP0 and S0NP3 presented the highest and lowest EL, respectively (Table 2). Based on present results, salinity stress decreased relative water content in plants, while the lowest RWCs were measured in S2NP0 and S2NP1. Foliar application of cerium oxide nanoparticles could improve the negative effects of salinity on RWC in treated plants (Table 3).

3.6. Mineral content analysis

As presented in Table 2, interaction between salinity with CeO_2 NPs affected only content of Cl and Ca as well as Na^+/K^+ ratio. Concerning Ca^{2+} content, S0NP1 and S2NP1 exhibited the highest and lowest content of Ca in treated plants, respectively. The rate of increase and decrease of Ca was 9.6% and 54.2% for S0NP1 and S2NP1, respectively. In the case of Cl, the highest and lowest contents were detected in plants exposed to S2NP0 and S0NP2, respectively. A 3.4-fold increase and a 1.4-fold decrease were noted in the mentioned treatments. Concerning our results, salinity led to a significant decrease in P content of treated plants (Fig. 3d).

The maximum concentration of salinity treatment (75 mM NaCl) resulted in the highest level of Na, while increasing CeO_2 NP concentrations (0–100 mg L^{-1}) lowered Na content (Fig. 3e). However, the interaction between salinity and CeO_2 NPs was not significant ($p = 0.879$). With increasing the concentration of both salinity and CeO_2 NP treatments, the content of K was decreased. However, we observed a weak increment of K in plants treated by 25 mg L^{-1} CeO_2NPs (Fig. 3f).

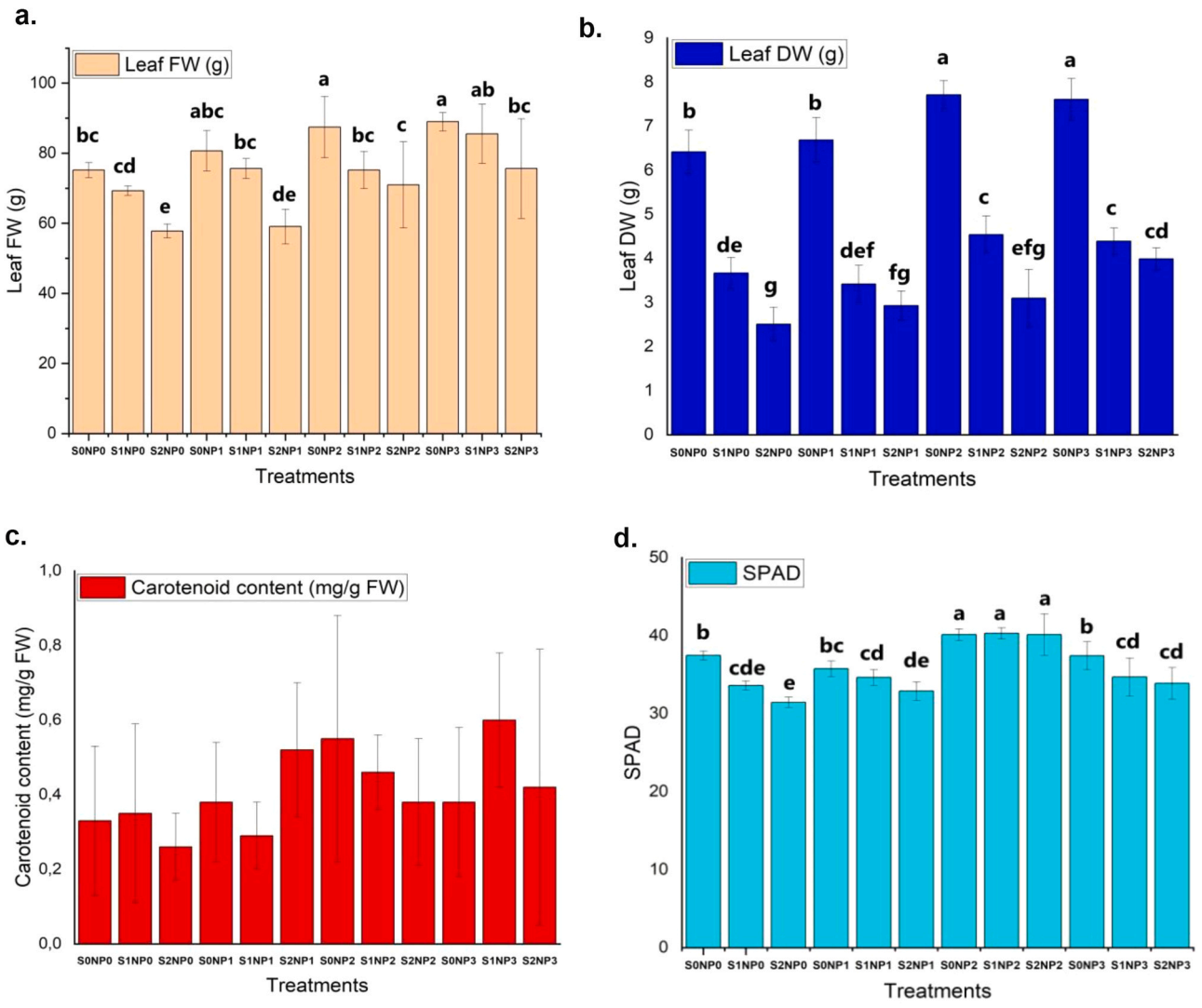

Fig. 2. Leaf FW (a), Leaf DW (b), Carotenoid content (c) and SPAD (d) values corresponding to treatments of CeO_2 nanoparticle and salinity stress in *Vitis vinifera* cv. Flame Seedless. Different letters indicate significant differences based on Duncan's post-hoc analysis at $p \leq 0.05$.

Table 2
Effects of CeO_2 nanoparticles and salinity application on leaf number, leaf area, plant height and photosynthesis pigments in *Vitis vinifera* cv. Flame Seedless.

Treatment	Leaf number	Leaf area (cm^2)	Plant height (cm)	Chl*a* (mg g^{-1}FW)	Chl*b* (mg g^{-1}FW)
S0NP0	13.50 ± 1.29**bcd**	39.89 ± 1.15**b**	48.46 ± 0.72 **c**	4.74 ± 0.58**c**	1.72 ± 0.30**b**
S1NP0	11.75 ± 0.96 **d**	33.23 ± 0.90**ef**	43.92 ± 1.40**d**	3.79 ± 0.39**d**	1.20 ± 0.12**d**
S2NP0	5.50 ± 0.58**f**	30.82 ± 0.87**g**	34.84 ± 1.39**g**	2.71 ± 0.71**e**	0.65 ± 0.21**g**
S0NP1	15.50 ± 1.29**b**	36.70 ± 1.87**d**	50.95 ± 1.36**b**	4.63 ± 0.31**c**	1.45 ± 0.14 **c**
S1NP1	15.00 ± 1.15**bc**	34.88 ± 0.74**e**	45.63 ± 1.47**d**	3.52 ± 0.24**d**	1.11 ± 0.09**de**
S2NP1	6.50 ± 1.29**f**	32.56 ± 1.66**f**	39.61 ± 0.87**f**	2.41 ± 0.36**e**	0.69 ± 0.12**g**
S0NP2	18.00 ± 0.82**a**	43.18 ± 1.73**a**	55.41 ± 1.73**a**	6.22 ± 0.27**a**	2.51 ± 0.20**a**
S1NP2	12.75 ± 1.26**d**	37.54 ± 0.70**d**	48.58 ± 0.89**c**	5.41 ± 0.29**b**	1.79 ± 0.05**b**
S2NP2	9.25 ± 1.26**e**	34.40 ± 0.56**e**	41.86 ± 0.54**e**	3.61 ± 0.55**d**	0.96 ± 0.11**ef**
S0NP3	18.00 ± 2.16 **a**	43.18 ± 0.59 **a**	53.69 ± 1.11**a**	2.87 ± 0.15**e**	0.75 ± 0.08**fg**
S1NP3	13.25 ± 1.50 **cd**	39.39 ± 0.70**bc**	49.12 ± 1.60**bc**	2.69 ± 0.32**e**	0.61 ± 0.10**g**
S2NP3	9.00 ± 1.83**e**	38.09 ± 0.55**cd**	38.59 ± 1.72**f**	2.42 ± 0.32**e**	0.51 ± 0.14**g**

Different letters indicate significant differences based on Duncan's post-hoc analysis at p ≤ 0.05.

Similar to observed results on the level of Na, the maximum and minimum Na/K was recorded by the highest concentration of salinity and CeO_2 NP treatments (75 Mm and 100 mg L^{-1}), respectively.

3.7. Malondialdehyde (MDA) and H_2O_2 quantification

MDA content was significantly affected by salinity, CeO_2 NPs and their interactions ($p = 0.0001$). S2NP0 and S0NP3 resulted in the maximum and minimum accumulation of MDA, respectively. A decrease of 4.6% in MDA content was recorded in plants treated with CeO_2 NPs in comparison with control samples (Table 4). Salinity and CeO_2 NPs treatments alone caused significantly increases in H_2O_2 content ($p = 0.0001$), but their interactive effect was not significant ($p = 0.738$). Plant exposure to 75 mM NaCl significantly increased H_2O_2 content

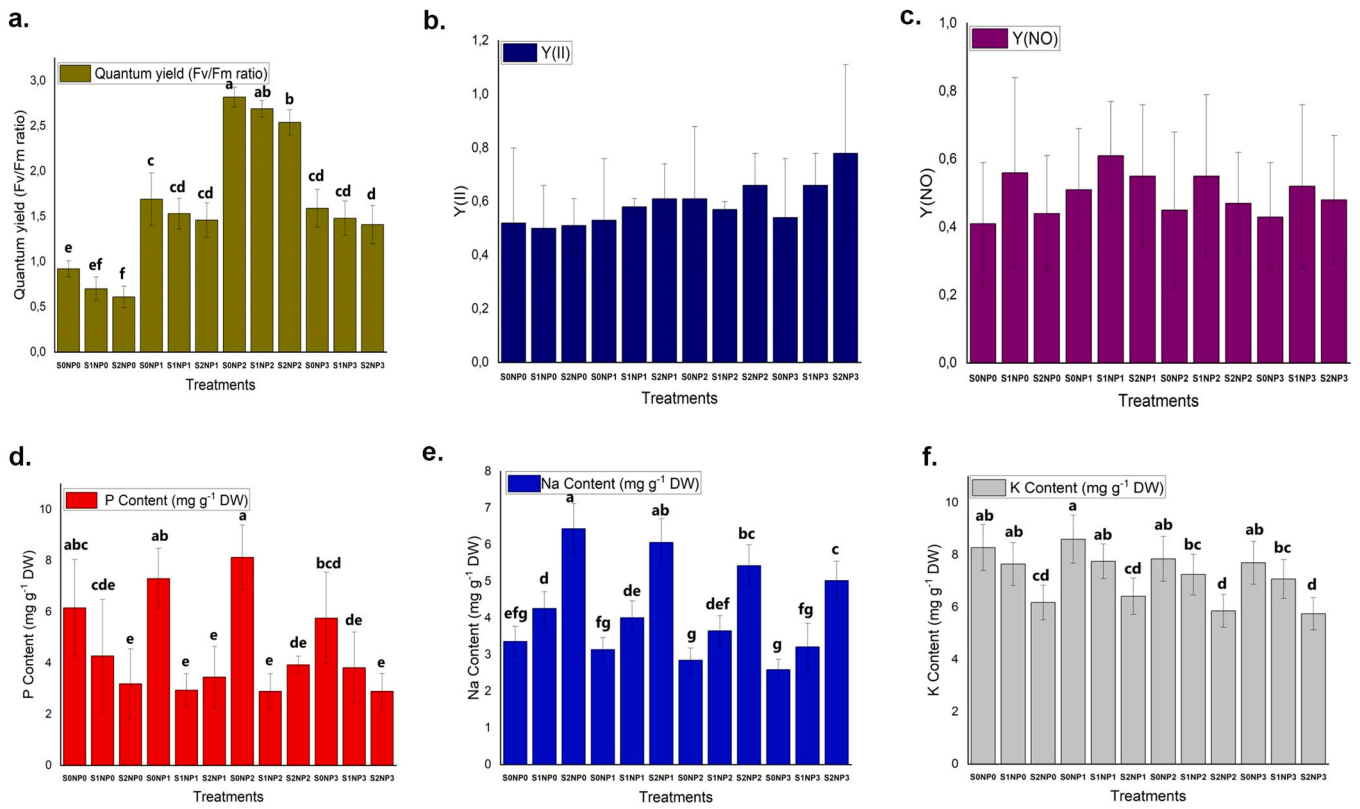

Fig. 3. $^{Fv}/_{Fm}$ (a), Y(II) (b) and Y(NO) (c), P content (d), Na content (e) and K content (f) values corresponding to treatments ofCeO_2 nanoparticles and salinity stress in *Vitis vinifera* cv. Flame Seedless. Different letters indicate significant differences based on Duncan's post-hoc analysis at $p \leq 0.05$.

Table 3
Effects of CeO_2 nanoparticles and salinity application on EL, RWC and elemental uptake in *Vitis vinifera* cv. Flame Seedless.

Treatment	EL (%)	RWC (%)	Cl (mg g^{-1}DW)	Ca (mg g^{-1}DW)	Na/K
S0NP0	17.75 ± 0.96**g**	76.36 ± 1.97 **a**	2.57 ± 0.38 **ef**	4.29 ± 0.20 **b**	0.40 ±0.01**g**
S1NP0	27.50 ± 1.29**d**	71.22 ± 0.31**f**	3.77 ± 0.38 **c**	3.28 ± 0.27 **d**	0.56 ± 0.00 **d**
S2NP0	50.25 ± 1.50**a**	68.05 ± 0.12**g**	8.30 ± 0.28 **a**	2.06 ± 0.10 **e**	1.04 ± 0.00 **a**
S0NP1	14.25 ±1.26**h**	74.45 ± 0.50 **bc**	2.31 ± 0.45 **fg**	4.69 ± 0.36 **a**	0.36 ±0.00**h**
S1NP1	24.25 ± 1.50**e**	71.87 ± 0.20 **ef**	3.39 ± 0.40**cd**	3.31 ± 0.38 **d**	0.52 ± 0.02 **e**
S2NP1	45.25 ± 2.50**b**	66.03 ± 0.59**h**	8.02 ± 0.13 **a**	1.96 ± 0.24 **e**	0.95 ± 0.00 **b**
S0NP2	13.50 ± 1.73**h**	75.50 ±0.48**ab**	1.84 ± 0.33**g**	4.14 ± 0.20**bc**	0.36 ±0.01**h**
S1NP2	21.50 ± 1.29**f**	73.65 ±0.43**cd**	2.86 ± 0.34 **de**	3.48 ± 0.28 **d**	0.50 ± 0.00 **e**
S2NP2	35.50 ± 0.58 **c**	70.89 ± 0.43**f**	6.66 ± 0.46 **b**	2.12 ± 0.14 **e**	0.93 ± 0.01 **b**
S0NP3	12.75 ± 1.71**h**	74.57 ± 1.14 **bc**	2.03 ± 0.15 **fg**	4.22 ± 0.21 **bc**	0.34 ± 0.00**i**
S1NP3	23.00 ± 1.63 **ef**	71.91 ± 1.50 **ef**	3.27 ± 0.38**cd**	3.91 ± 0.09 **c**	0.45 ± 0.05**f**
S2NP3	36.75 ± 1.71 **c**	72.79 ± 1.11 **de**	6.73 ± 0.50 **b**	2.06 ± 0.16 **e**	0.87 ± 0.00 **c**

Different letters indicate significant differences based on Duncan's post-hoc analysis at $p \leq 0.05$.

Table 4
Effects of CeO_2 nanoparticles and salinity application on MDA, H_2O_2, Proline, GP, APX, and SOD activities in *Vitis vinifera* cv. Flame Seedless.

Treatment	MDA (nM g^{-1} FW)	H_2O_2 (μMol g^{-1} FW)	Proline (μM g^{-1} FW)	GP (U g^{-1} FW)	APX (U g^{-1} FW)	SOD (U g^{-1} FW)
S0NP0	8.21 ± 0.32**f**	16.15 ± 0.26 **f**	0.06 ± 0.03 **e**	163.34 ± 13.30 **f**	233.65 ± 2.61 **d**	4.26 ± 0.48 **d**
S1NP0	11.55 ± 0.44 **d**	27.27 ± 0.79 **cd**	0.17 ± 0.03 **d**	225.75 ± 18.39 **de**	245.95 ± 3.01 **c**	7.63 ± 0.87 **c**
S2NP0	23.99 ± 0.92 **a**	38.13 ± 2.17 **b**	0.26 ± 0.04 **c**	236.14 ± 19.23 **d**	244.57 ± 2.34 **c**	14.73 ± 1.67 **b**
S0NP1	8.05 ± 0.31**f**	16.57 ± 0.83 **f**	0.12 ± 0.02 **de**	160.08 ± 13.04 **f**	256.11 ± 2.70 **b**	4.38 ± 0.50 **d**
S1NP1	11.32 ± 0.43 **d**	26.79 ± 1.29 **d**	0.33 ± 0.05 **c**	221.23 ± 18.02 **de**	255.46 ± 3.21 **b**	7.88 ± 0.88 **c**
S2NP1	23.50 ± 0.91 **a**	37.78 ± 1.51 **b**	0.48 ± 0.08 **b**	231.41 ± 18.85 **d**	258.89 ± 0.93 **b**	15.17 ± 1.72 **b**
S0NP2	8.26 ± 0.32 **f**	19.32 ± 1.05 **e**	0.13 ± 0.03 **de**	196.01 ± 15.96 **e**	275.07 ± 3.72 **a**	4.34 ± 0.49 **d**
S1NP2	10.86 ± 0.42 **d**	28.67 ± 1.18 **c**	0.35 ± 0.06 **c**	270.90 ± 22.06 **c**	276.28 ± 2.14 **a**	7.77 ± 0.88 **c**
S2NP2	22.54 ± 0.86 **b**	40.72 ± 0.98 **a**	0.52 ± 0.08 **b**	283.36 ± 23.08 **bc**	279.06 ± 1.67 **a**	15.01 ± 1.71 **b**
S0NP3	7.83 ± 0.30 **f**	16.36 ± 0.62 **f**	0.13 ± 0.03 **de**	223.78 ± 18.23 **de**	254,75 ± 5,31 **b**	4.90 ± 0.56 **d**
S1NP3	9.24 ± 0.36 **e**	25.92 ± 0.73 **d**	0.52 ± 0.08 **b**	309.27 ± 25.19 **ab**	255.78 ± 4.72 **b**	8.77 ± 1.00 **c**
S2NP3	19.19 ± 0.73 **c**	36.97 ± 1.67 **b**	0.78 ± 0.13 **a**	323.52 ± 26.35 **a**	256.69 ± 4.99 **b**	16.94 ± 1.92 **a**

Different letters indicate significant differences based on Duncan's post-hoc analysis at $p \leq 0.05$.

compared with controls. Contrarily, plants exposed to CeO_2 NP treatments displayed different trend. CeO_2 NPs at 100 mg L^{-1} had the most pronounced impact on decreasing H_2O_2 content in relation with control samples (Table 4).

3.8. Proline content

Proline content was influenced by salinity, CeO_2 NPs and their interaction. Both salinity and its combination with NPs caused higher increases in proline content in comparison with NP treatments alone highest and lowest proline contents were recorded in S2NP3 and control groups, respectively (Table 4).

3.9. Antioxidant enzyme activities

In regard with the antioxidant defence apparatus, SOD enzymatic activity was significantly affected by both salinity and CeO_2 NP treatments, but their interaction was not significant ($p = 0.886$). Both salinity and CeO_2 NPs increased SOD activity, with highest levels recorded at 75 mM salinity and 100 mg L^{-1} CeO_2 NPs (Table 4). Concerning APX activity, salinity, CeO_2 NPs and their interactions all resulted in significant regulation. Specifically, highest and lowest APX activity was recorded in plants exposed to S2NP2 and controls, respectively. In a similar fashion to SOD, GP activity increased following both salinity and CeO_2 NP treatments, with salt-stressed samples at 75 mM NaCl displaying highest GP activity levels (Table 4).

3.10. Heat map clustering and principal component analysis (PCA)

A heat map was constructed in order to visualize, clarify and associate the findings along with the experimental groups. According to the clustering of heat map, treatments of the different combinations of nanoparticles and different salinity levels were clearly classified into three distinct groups. Herewith, the first cluster included S2NP0, S2NP1, S2NP2, and S2NP3. The second cluster was composed of S1NP0, S1NP1, S1NP2, and S1NP3, while the non-stressed, NP-treated sample groups were clearly separated in the third cluster. On the other hand, the evaluated variables were classified into two main groups (Fig. 4a). Specifically, proline, GP, EL, Na, MDA, Na/K, Cl, H_2O_2, SOD, Y (II), and Y (NO) were classified into the first cluster and the relevant values of those variables were significantly increased by salinity stress in comparison with non-stressed, NP-treated plants. Other variables relating agronomic traits and photosynthesis machinery apparatus traits were significantly decreased due the salinity but the highest values of these components were recorded under both control and NP-treated groups.

For the overall assessment of agronomic traits, physiological attributes, nutrient uptake, and enzymatic activities, experimental data were subjected to PCA. Four principal components with Eigenvalues > 1.0, accounted for 92.17% of the variability of the original data. Such a high explained variance ratio of the components suggested that the evaluated variables along with the treatments could be strongly explained with the relevant component analysis. The first principal component, PC1, accounting for 60.89% of total variation, exhibited significant positive correlations with leaf FW, leaf DW, leaf number, leaf area, plant height, SPAD, Chl *a*, Chl *b*, RWC, P, and Ca. The first component was regarded as yield traits and biochemical parameters. On the other hand, in the second principal component, PC2, accounting for16.36% of the total variation, Y(II), $^{Fv}/_{Fm}$, carotenoid, proline, GP,and APX had higher Eigenvectors. Herein, the second component included photosynthesis machinery apparatus and enzymatic activity-related parameters. According to the scores of the first two components, experimental groups were scattered in a biplot (Fig. 4b, c).

4. Discussion

Soil salinization is one of the major threats to crops worldwide, quickly limiting water uptake and subsequently causing osmotic stress as during drought but additionally accumulating ions leading to ionic stress (Munns and Tester, 2008; Lamers et al., 2020). As previously observed for most plant species (Ren et al., 2020; Tanveer et al., 2020) in general, and grapevine in particular (A.A. Mozafari et al., 2018; A A AA Mozafari et al., 2018; Upadhyay et al., 2018), slow and retarded growth under higher levels of soil salinity have been reported. Due to poor public perception of genetically modified crops in many regions, the use of nanoparticles has gained increasing interest as a potential and excellent alternative tool to alleviate stress damage in plants (Ioannou et al., 2020; Zulfiqar and Ashraf, 2021) and significant and clear outputs have been obtained in a dose-dependent manner (Gohari et al., 2020b). Even though some progress has been made concerning physiological, biochemical as well as molecular responses, current overall knowledge regarding mechanisms of action remains at an infancy stage (Zulfiqar and Ashraf, 2021). Of the investigated NPs, cerium oxide NPs have been reported to exhibit positive effects in plants (Corral-Diaz et al., 2014; Wang et al., 2019, 2020; Jahani et al., 2019), but research on CeO_2 NPs towards enhanced salinity tolerance in crop plants is limited (Zulfiqar and Ashraf, 2021). For that reason, the current study assessed the interaction between CeO_2 NPs and salinity stress in *Vitis vinifera* cv. Flame Seedless. Grapevine, as a major commercial fruit crop, is mostly grown in areas characterized by salinity problems, which cause reductions in yield and quality of the fruits (Upadhyay et al., 2018). In accordance with the conditions of the region and sensitivity of grapevine cultivars to salinity, we investigated the possible and potential uses of CeO_2 NPs in diminishing the negative impacts of salinity.

Herein, according to the phenotypic observation of the plants (data not shown), foliar spraying of CeO_2 NPs caused substantial, positive impacts in treated plants in comparison with control and salt-stressed ones. Current findings demonstrate that salinity decreased FW and DW of grapevine plants, which is consistent with the results of Acosta-Motos et al. (2017), but corresponding values increased along with increasing concentrations of CeO_2 NPs. Similar increases in FW and DW in other plant species in response to CeO_2 NP treatment have been reported (Skiba et al., 2020; Jurkow et al., 2020). A significant decline observed in RWC affected by both salinity and CeO_2 NP application may be due to the plant's defence strategies to mitigate NP uptake following NP translocation pathways through water flows (Schwabe et al., 2013). In addition, NP-exposed leaves have exhibited up-regulation of some transcription factors, which are considered to play significant roles concerned with reproductive and vegetative development of Arabidopsis plants (Tumburu et al., 2017).

Chlorophyll fluorescence responses are a powerful tool to investigate the physiology of plants under stress conditions such as salinity. Under salt stress, decrease in chlorophyll fluorescence occurs due to decline of photosynthetic efficiency. Some reports suggest that application of nanoparticles could promote the light energy absorbed from PSI and transformed to PSII, and induce electron transport (Jurkow et al., 2020; Tombuloglu et al., 2020). Regarding current results, CeO_2 NP treatment ($p = 0.0001$), low concentrations presented a stimulatory effect on the contents of Chl *a* and *b*. Similar enhancement was previously reported following treatment with low concentration of CeO_2 NPs (Gui et al. (2017), in agreement with current findings. Data regarding Chl *a* and Chl *b* contents were consistent with high values of leaf number, leaf area and plant height and low values of membrane damage, which suggest chlorophyll as being critical in enhancing biomass (Gui et al., 2017). In addition, catalytic properties of cerium relating chlorophyll biosynthesis and chloroplast structure maintenance have been reported (Shyam and Aery, 2012; Chen et al., 2015). According to current findings, highest concentration of CeO_2 NPs caused significant decreases in Chl *a* and *b* concentration. Ma et al. (2013) and Singh et al. (2019) postulated that relevant decreases might be the consequence of nanoceria transformation inside plant tissues.

Chlorophyll fluorescence-related parameters are widely used and accepted tools in order to estimate the photosynthetic activity of the

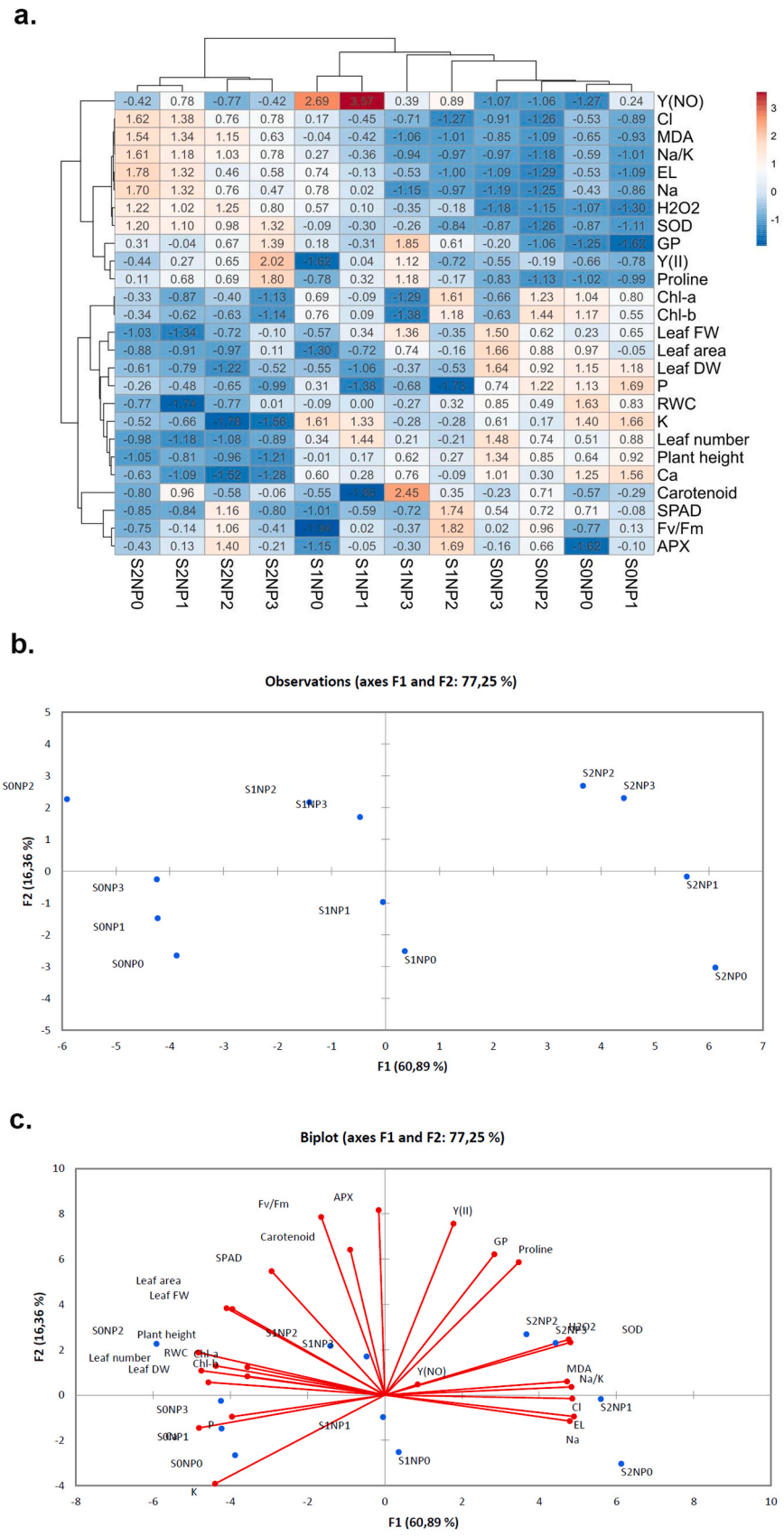

Fig. 4. Heat maps corresponding to the dependent and independent variables along with the treatments (a), principal component analysis regarding observations (a) and biplot (b) (PCA) of salinity and CeO_2 nanoparticles application on the examined traits in *Vitis vinifera* cv. Flame Seedless.

plant (Maxwell and Johnson, 2000). $^{Fv}/_{Fm}$ acts as an indicator of the PSII photosynthetic energy conversion, and reflects the light reemission by chlorophyll molecules when light returns from excited state to ground state (Maxwell and Johnson, 2000). Under stress conditions, substantial decreases are noted in electron flux from PSII to the quinone acceptor, and subsequently reductions in $^{Fv}/_{Fm}$ values. Along with those decreases, critical reductions in photosynthesis occur (Baker and Rosenqvist, 2004) as previously reported for a large number of plant species, with salinity leading to reduced $^{Fv}/_{Fm}$ ratio, indicating negative impacts on photoreceptor centres (Kafi et al., 2019). An enhanced $^{Fv}/_{Fm}$ ratio was recorded in plants treated with CeO_2 NPs, consistent with the report by Rossi et al. (2016), which might be explained through CeO_2 NP-mediated enhancements in light energy use efficiency of PSII in plants under salinity stress. Similarly, Arabidopsis plants embedded with poly (acrylic acid) cerium oxide nanoparticles that were exposed to abiotic stress exhibited an increase up to 19% in quantum yield of photosystem II (Wu et al., 2017).

Electrolyte leakage can be used as a useful damage indicator to detect the rate of injury in cell membrane under salt stress conditions, being the primary site of ion-specific damage due to salinity (Hniličková et al., 2019). Plants with low EL indexes are considered to be tolerant against stress. As clearly documented for several other plant species (Hniličková et al., 2019; Mahlooji et al., 2018; Hatami et al., 2018), current findings revealed that salinity increased EL from plasma membranes, but leakage was attenuated with lower concentrations of CeO_2 NP treatments.

To investigate the impact of CeO_2 NPs in salt-stressed plants, proline accumulation was analysed. As a common osmolyte in water- and salt-stressed plants (Jiménez-Bremont et al., 2006; Tripathi et al., 2007), proline has a vital role in protein protection against denaturation (Hong et al., 2000) and scavenging reactive oxygen species (ROS). Both antioxidant and oxidative stress inducer role of CeO_2 NPs have been previously demonstrated, depending on the size and surface properties, plant age, and exposure duration (Ma et al., 2016a, 2016b). Increase in proline accumulation in plants treated with CeO_2 NPs may contribute to stabilizing sub-cellular structures and osmotic balance in the cytosol. The higher accumulation of proline found in plants exposed to higher concentrations of CeO_2 NPs, may be linked with increase capacity of scavenging free radicals and protecting cells from oxidative damage as a stress protection mechanism (Wang et al., 2020).

In regard with the antioxidant response, salinity lead to an increase in H_2O_2 content, as well as GP and SOD enzymatic activities. It is well known that CAT, SOD, GP, and APX act as a defence mechanism for ROS detoxification under salinity (Hasanuzzaman et al., 2020). Concordantly, stress-mediated production of H_2O_2 is a key indicator of problematic cellular integrity, which in turn results in oxidative damage to plants (Wang et al., 2019). In the case of inefficient reduction or scavenging by the relevant plant antioxidant enzymes, an over-production of H_2O_2 is commonly observed under high levels of salinity (AbdelLatef et al., 2018; Abdelaal et al., 2020). Furthermore, disturbance in timing required to activate antioxidant enzymes in order to coordinate with the production of ROS results in over-production of H_2O_2 (AbdelLatef et al., 2018). As reported by Korsvik et al. (2007) and Hussain et al. (2017), a main protective role has been attributed to the ceria nanoparticles thanks to their SOD mimetic activity. Furthermore, ceria NPs are characterized with a peculiar unique surface redox chemistry, which induces substantial biochemical and physiological function in plants (Rico et al., 2017). Considering SOD activity, all concentrations of CeO_2 NP treatments did not significantly affect SOD activity under non-saline conditions, whilst SOD activity increased under both salinity and CeO_2 NP treatments. SOD dismutates ROS to H_2O_2 and this is subsequently converted to H_2O through the activities of CAT, APX, GPX and other antioxidant enzymes (Hussain et al., 2019). According to the current findings, SOD activity is positively correlated with H_2O_2 content ($p < 0.001$; $r = 0.959$). In the current experimental setup, salinity increased H_2O_2 content but plants did not respond accordingly to the low concentration of CeO_2NP treatments, relative to the control plants. In accordance with H_2O_2 content, no significant correlations were observed with APX and GP with H_2O_2 content. However, in the study by Rico et al. (2013), concentrations of 62.5 and 125 mg CeO_2NPs L^{-1} lowered H_2O_2content in rice but higher concentration of CeO_2NPs did not affect H_2O_2 content significantly. Cerium oxide nanoparticles with low Ce^{3+}/Ce^{4+} ratio (35%) reduced the levels of leaf ROS (by 52%), including H_2O_2 (Wu et al., 2017).

As reported for most plant species, abiotic stress factors in general, and salinity in particular, damage plants through over-generation of ROS due to oxidative stress. MDA content is widely assayed for estimating the membrane lipid damage of plant cells (Wang et al., 2019). Current findings revealed significant damage with increasing salinity levels in grapevine, directly linked to stress-mediated lipid peroxidation that resulted in disturbed membrane integrity and increased MDA content. Similar to the effect of other NPs (Askary et al., 2017; Mohamed et al., 2017), CeO_2 NPs decreased MDA content, suggesting the capability of CeO_2NP application on promoting plant tolerance to salinity stress. This capability may also be explained with the non-toxic concentration of the applied NPs; however, current results are not in agreement with those by Rico et al. (2013), who demonstrated increased MDA content and ion leakage in rice shoots following CeO_2 NP treatment. Observed differences are likely to be dependent on plant growth conditions, plant species, and exposure concentration and duration (Ma et al., 2016b, 2016a; Wang et al., 2012).

Concerning the smooth running of metabolic processes in plants including defence responses, uptake, partitioning and interactions of minerals in plant tissues are of fundamental importance. In the case of salt stress response and depending on the salinity level or duration, substantial deviations from the optimal levels of minerals have been reported for a large number of plants species (Yildirim et al., 2006; Wu et al., 2013; Borrelli et al., 2018). K^+ retention in plant cells is known as a mechanism to improve salinity stress tolerance in crops (Ismail and Horie, 2017). Previous results showed that CeO_2 NPs assist in the higher retention of K^+ in leaf mesophyll, resulting in improving plant photosynthetic performance under environmental stimuli such as salinity (Boghossian et al., 2013a, 2013b; Wu et al., 2017, 2018). Similar to other findings, our results showed that application of CeO_2 NPs could decrease damaging sodium uptake in grapevine plants. Rossi et al. (2017) stated that CeO_2 NPs treatment reduced root apoplastic barriers which permitted more Na^+ transport to shoots and less Na^+ accumulation in salt-stressed plant roots.

5. Conclusion

Application of CeO_2 NPs provided significant protection to grapevine plants exposed to salinity stress, highlighting the promising role of nanomaterials in agriculture. This was revealed through the improvement of various agronomic, physiological and biochemical parameters. Nonetheless, further studies are needed in order to reveal the exact modus operandi of ceria nanoparticles in organs of grapevine plants. In that context, the uptake, translocation and partitioning of cerium concentrations deserves thorough examination, while systems biology approaches could provide useful insight into regulatory components involved in stress responses. Furthermore, in addition to the potted plant experiments carried out under controlled conditions, follow-up field trials could contribute to the understanding of potential applications of these advanced nanoparticles in agriculture under ever-changing environmental conditions, at the same time examining potential memory/trans-generational effects that may occur due to possible epigenetic modifications.

Ethics approval and consent to participate

We confirm that our study does not involve human subjects.

Funding

This research did not receive any specific grant from funding agencies in the public, commercial, or not-for-profit sectors.

CRediT authorship contribution statement

All authors have contributed to carry out this research. GG and VF designed the experimental setup. HR and HF performed greenhouse experiments, biochemical and physiological parameters. MA and HB synthesized and characterized nanomaterials, EZ and MK performed statistical analysis. GG, EZ, SP and MK analysed data and results and wrote the first draft, while GG, MK, MM and VF wrote and edit the final manuscript. All authors read and approved the final manuscript.

Declaration of Competing Interest

The authors declare that they have no competing interests.

Data Availability

The data that support the findings of this study are available from the corresponding author upon reasonable request.

Acknowledgments

We would like to thank University of Maragheh, Iran for their supports during this project.

Appendix A. Supporting information

Supplementary data associated with this article can be found in the online version at doi:10.1016/j.ecoenv.2021.112402.

References

Abdelaal, K.A., Mazrou, Y.S., Hafez, Y.M., 2020. Silicon foliar application mitigates salt stress in sweet pepper plants by enhancing water status, photosynthesis, antioxidant enzyme activity and fruit yield. Plants (Basel Switz.) 9 (6), 733.

AbdElgawad, H., Zinta, G., Hegab, M.M., Pandey, R., Asard, H., Abuelsoud, W., 2016. High salinity induces different oxidative stress and antioxidant responses in maize seedlings organs. Front. Plant Sci. 7, 276.

AbdelLatef, A.A.H., Srivastava, A.K., El-sadek, M.S.A., Kordrostami, M., Tran, L.-S.P., 2018. Titanium dioxide nanoparticles improve growth and enhance tolerance of broad bean plants under saline soil conditions. Land Degrad. Dev. 29, 1065–1073.

Acosta-Motos, J.R., Ortuño, M.F., Bernal-Vicente, A., Diaz-Vivancos, P., Sanchez-Blanco, M.J., Hernandez, J.A., 2017. Plant responses to salt stress: adaptive mechanisms. Agronomy 7 (1), 18.

Amini, Mojtaba, Hassandoost, Ramin, Bagherzadeh, Mojtaba, Gautam, Sanjeev, Chae, Keun Hwa, 2016. "Copper nanoparticles supported on CeO2 as an efficient catalyst for click reactions of azides with alkynes. Catal. Commun. 85, 13–16.

Askary, M., Talebi, S.M., Amini, F., Bangan, A.D.B., 2017. Effects of iron nanoparticles on Menthapiperita L. under salinity stress. Biologia 63 (1).

Baker, N.R., Rosenqvist, E., 2004. Applications of chlorophyll fluorescence can improve crop production strategies: an examination of future possibilities. J. Exp. Bot. 55, 1607–1621.

Bates, L.S., Waldren, R.P., Teare, I.D., 1973. Rapid determination of free proline for water-stress studies. Plant Soil 39 (1), 205–207.

Boghossian, A.A., Sen, F., Gibbons, B.M., Sen, S., Faltermeier, S.M., Giraldo, J.P., Strano, M.S., 2013a. Application of nanoparticle antioxidants to enable hyperstable chloroplasts for solar energy harvesting. Adv. Energy Mater. 3 (7), 881–893.

Boghossian, A.A., Sen, F., Gibbons, B.M., Sen, S., Faltermeier, S.M., Giraldo, J.P., Zhang, C.T., Zhang, J., Heller, D.A., Strano, M.S., 2013b. Application of nanoparticle antioxidants to enable hyperstable chloroplasts for solar energy harvesting. Adv. Energy Mater. 3, 881–893.

Borrelli, G.M., Fragasso, M., Nigro, F., Platani, C., Papa, R., Beleggia, R., Trono, D., 2018. Analysis of metabolic and mineral changes in response to salt stress in durum wheat (Triticum turgidum ssp. durum) genotypes, which differ in salinity tolerance. Plant Physiol. Biochem. 133, 57–70.

Bradford, M.M., 1976. A rapid and sensitive method for the quantitation of microgram quantities of protein utilizing the principle of protein-dye binding. Anal. Biochem. 72 (1–2), 248–254.

Chen, Y., Luo, Y., Qiu, N., Hu, F., Sheng, L., Wang, R., Cao, F., 2015. Ce 3+ induces flavonoids accumulation by regulation of pigments, ions, chlorophyll fluorescence and antioxidant enzymes in suspension cells of Ginkgo biloba L. Plant Cell, Tissue Organ Cult. (PCTOC) 123 (2), 283–296.

Corral-Diaz, B., Peralta-Videa, J.R., Alvarez-Parrilla, E., Rodrigo-García, J., Morales, M.I., Osuna-Avila, P., Gardea-Torresdey, J.L., 2014. Cerium oxide nanoparticles alter the antioxidant capacity but do not impact tuber ionome in Raphanus sativus (L). Plant Physiol. Biochem. 84, 277–285.

Fisarakis, I., Chartzoulakis, K., Stavrakas, D., 2001. Response of Sultana vines (V. vinifera L.) on six rootstocks to NaCl salinity exposure and recovery. Agric. Water Manag. 51, 13–27.

Flohe, L., Günzler, W.A., 1984. Assays of glutathione peroxidase. Method Enzym. 105, 114–120.

Fraga, H., Malheiro, A.C., Moutinho-Pereira, J., Santos, J.A., 2012. An overview of climate change impacts on European viticulture. Food Energy Secur. 1, 94–110.

Ghosh, K., 1993. Methods of analysis of soils, plants, waters and fertilizers. J. Ind. Soc. Soil Sci. 41 (4), 814–815.

Gohari, G., Mohammadi, A., Akbari, A., Panahirad, S., Dadpour, M.R., Fotopoulos, V., Kimura, S., 2020a. Titanium dioxide nanoparticles (TiO2 NPs) promote growth and ameliorate salinity stress effects on essential oil profile and biochemical attributes of Dracocephalum moldavica. Sci. Rep. 10 (1), 1–14.

Gohari, G., Safai, F., Panahirad, S., Akbari, A., Rasouli, F., Dadpour, M.R., Fotopoulos, V., 2020b. Modified multiwall carbon nanotubes display either phytotoxic or growth promoting and stress protecting activity in Ocimum basilicum L. in a concentration-dependent manner. Chemosphere 249, 126171.

Gui, X., Rui, M., Song, Y., Ma, Y., Rui, Y., Zhang, P., He, X., Li, Y., Zhang, Z., Liu, L., 2017. Phytotoxicity of CeO2 nanoparticles on radish plant (Raphanus sativus). Environ. Sci. Pollut. Res. 24 (15), 13775–13781.

Hasanuzzaman, M., Bhuyan, M.H.M., Zulfiqar, F., Raza, A., Mohsin, S.M., Mahmud, J.A., Fotopoulos, V., 2020. Reactive oxygen species and antioxidant defense in plants under abiotic stress: revisiting the crucial role of a universal defense regulator. Antioxidants 9 (8), 681.

Hatami, E., Shokouhian, A.A., Ghanbari, A.R., Naseri, L.A., 2018. Alleviating salt stress in almond rootstocks using of humic acid. Sci. Hortic. 237, 296–302.

Hniličková, H., Hnilička, F., Orsák, M., Hejnák, V., 2019. Effect of salt stress on growth, electrolyte leakage, Na+ and K+ content in selected plant species. Plant Soil Environ. 65 (2), 90–96.

Hong, Z., Lakkineni, K., Zhang, Z., Verma, D.P.S., 2000. Removal of feedback inhibition of Δ1-pyrroline-5-carboxylate synthetase results in increased proline accumulation and protection of plants from osmotic stress. Plant Physiol. 122 (4), 1129–1136.

Hussain, I., Singh, N.B., Singh, A., Singh, H., Singh, S.C., Yadav, V., 2017. Exogenous application of phytosynthesized nanoceria to alleviate ferulic acid stress in Solanum lycopersicum. Sci. Hortic. 214 (2017), 158–164.

Hussain, I., Singh, A., Singh, N.B., Singh, A., Singh, P., 2019. Plant-nanoceria interaction: toxicity, accumulation, translocation and biotransformation. South Afr. J. Bot. 121 (2019), 239–247.

Ioannou, A., Gohari, G., Papaphilippou, P., Panahirad, S., Akbari, A., Dadpour, M.R., Krasia-Christoforou, T., Fotopoulos, V., 2020. Advanced nanomaterials in agriculture under a changing climate: the way to the future? Environ. Exp. Bot. 176, 104048.

Ismail, A.M., Horie, T., 2017. Genomics, physiology, and molecular breeding approaches for improving salt tolerance. Annu. Rev. Plant Biol. 68, 405–434.

Jahani, S., Saadatmand, S., Mahmoodzadeh, H., Khavari-Nejad, R.A., 2019. Effect of foliar application of cerium oxide nanoparticles on growth, photosynthetic pigments, electrolyte leakage, compatible osmolytes and antioxidant enzymes activities of Calendula officinalis L. Biologia 74 (9), 1063–1075.

Jiménez-Bremont, J.F., Becerra-Flora, A., Hernández-Lucero, E., Rodríguez-Kessler, M., Acosta-Gallegos, J.A., Ramírez-Pimentel, J.G., 2006. Proline accumulation in two bean cultivars under salt stress and the effect of polyamines and ornithine. Biol. Plant. 50 (4), 763–766.

Jurkow, R., Sękara, A., Pokluda, R., Smoleń, S., Kalisz, A., 2020. Biochemical response of oakleaf lettuce seedlings to different concentrations of some metal (oid) oxide nanoparticles. Agronomy 10 (7), 997.

Kafi, M., Nabati, J., Saadatian, B., Oskoueian, A., Shabahang, J., 2019. Potato response to silicone compounds (micro and nanoparticles) and potassium as affected by salinity stress. Ital. J. Agron. 14 (3), 162–169.

Korsvik, C., Patil, S., Seal, S., Self, W.T., 2007. Superoxide dismutase mimeticproperties exhibited by vacancy engineered ceria nanoparticles. Chem. Commun. 10, 1056–1058.

Kozminska, A., Hassan, Al, Hanus-Fajerska, M., Naranjo, E., Boscaiu, M.A., Vicente, O, M., 2018. Comparative analysis of water deficit and salt tolerance mechanisms in Silene. South Afr. J. Bot. 117, 193–206.

Kumar, D., Hassan, Al, Naranjo, M., Agrawal, M.A., Boscaiu, V., Vicente, O, M., 2017. Effects of salinity and drought on growth, ionic relations, compatible solutes and activation of antioxidant systems in oleander (Nerium oleander L.). PLoS One 12, 0185017.

Lamers, J., Van Der Meer, T., Testerink, C., 2020. How plants sense and respond to stressful environments. Plant Physiol. 182 (4), 1624–1635.

Ling, Q., Huang, W., Jarvis, P., 2011. Use of a SPAD-502 meter to measure leaf chlorophyll concentration in Arabidopsis thaliana. Photosynth Res. 107 (2), 209–214.

Ma, C., Chhikara, S., Xing, B., Musante, C., White, J.C., Dhankher, O.P., 2013. Physiological and molecular response of Arabidopsis thaliana (L.) to nanoparticles cerium and indium oxide exposure. ACS Sustain. Chem. Eng. 1 (7), 768–778.

Ma, X., Wang, Q., Rossi, L., Ebbs, S.D., White, J.C., 2016a. Multigenerational exposure to cerium oxide nanoparticles: physiological and biochemical analysis reveals transmissible changes in rapid cycling Brassica rapa. Nano Impact 1, 46–54.

Ma, X., Wang, Q., Rossi, L., Zhang, W., 2016b. Cerium oxide nanoparticles and bulk cerium oxide leading to different physiological and biochemical responses in Brassica rapa. Environ. Sci. Technol. 50, 6793–6802.
Mahlooji, M., Sharifi, R.S., Razmjoo, J., Sabzalian, M.R., Sedghi, M., 2018. Effect of salt stress on photosynthesis and physiological parameters of three contrasting barley genotypes. Photosynthetica 56 (2), 549–556.
Maxwell, K., Johnson, G.N., 2000. Chlorophyll fluorescence—a practical guide. J. Exp. Bot. 51, 659–668.
Mohamed, A.K.S., Qayyum, M.F., Abdel-Hadi, A.M., Rehman, R.A., Ali, S., Rizwan, M., 2017. Interactive effect of salinity and silver nanoparticles on photosynthetic and biochemical parameters of wheat. Arch. Agron. Soil Sci. 63 (12), 1736–1747.
Mohammadi, M.H.Z., Panahirad, S., Navai, A., Bahrami, M.K., Kulak, M., Gohari, G., 2021. Cerium oxide nanoparticles (CeO2-NPs) improve growth parameters and antioxidant defense system in Moldavian Balm (Dracocephalum moldavica L.) under salinity stress. Plant Stress 1, 100006. https://doi.org/10.1016/j.stress.2021.100006.
Mozafari, A.A., Ghaderi, N., 2018. Grape response to salinity stress and role of iron nanoparticle and potassium silicate to mitigate salt induced damage under in vitro conditions. Physiol. Mol. Biol. Plants 24 (1), 25–35.
Mozafari A.A., GhadakchiAsl A., Ghaderi N. 2018. Grape response to salinity stress and role of iron nanoparticle and potassium silicate to mitigate salt induced damage under in.
Munns, R., 2002. Comparative physiology of salt and water stress. Plant Cell Environ. 25, 239–250.
Munns, R., Tester, M., 2008. Mechanisms of salinity tolerance. Annu. Rev. Plant Biol. 59, 651–681.
Munns, R., Schachtman, D.P., Condon, A.G., 1995. The significance of a two-phase growth response to salinity in wheat and barley. Funct. Plant Biol. 22, 561–569.
Nakano, Y., Asada, K., 1981. Hydrogen peroxide is scavenged by ascorbate-specific peroxidase in spinach chloroplasts. Plant Cell Physiol. 22 (5), 867–880.
Nayyar, H., 2003. Accumulation of osmolytes and osmotic adjustment in water-stressed wheat (Triticum aestivum) and maize (Zea mays) as affected by calcium and its antagonists. Environ. ExpBot 50 (3), 253–264.
Ren, Y., Wang, W., He, J., Zhang, L., Wei, Y., Yang, M., 2020. Nitric oxide alleviates salt stress in seed germination and early seedling growth of pakchoi (Brassica chinensis L.) by enhancing physiological and biochemical parameters. Ecotoxicol. Environ. Saf. 187, 109785.
Rico, C.M., Hong, J., Morales, M.I., Zhao, L., Barrios, A.C., Zhang, J.Y., Gardea-Torresdey, J.L., 2013a. Effect of cerium oxide nanoparticles on rice: a study involving the antioxidant defense system and in vivo fluorescence imaging. Environ. Sci. Technol. 47 (11), 5635–5642.
Rico, C.M., Johnson, M.G., Marcus, M.A., Andersen, C.P., 2017. Intergenerational responses of wheat (Triticum aestivum L.) to cerium oxide nanoparticles exposure. Environ. Sci. Nano 4 (3), 700–711.
Ritchie, S.W., Nguyen, H.T., Holaday, A.S., 1990. Leaf water content and gas-exchange parameters of two wheat genotypes differing in drought resistance. Crop Sci. 30 (1), 105–111.
Rossi, L., Zhang, W., Lombardini, L., Ma, X., 2016. The impact of cerium oxide nanoparticles on the salt stress responses of Brassica napus L. Environ. Pollut. 219, 28–36.
Rossi, L., Zhang, W., Ma, X., 2017. Cerium oxide nanoparticles alter the salt stress tolerance of Brassica napus L. by modifying the formation of root apoplastic barriers. Environ. Pollut. 229, 132–138.
Ryan, J., Estefan, G., Rashid, A., 2001. Soil and Plant Analysis Laboratory Manual. ICARDA.
Schwabe, F., Schulin, R., Limbach, L.K., Stark, W., Bürge, D., Nowack, B., 2013. Influence of two types of organicmatter on interaction of CeO_2 nanoparticles with plants in hydroponic culture. Chemosphere 91, 512–520.
Sharma, P., JhaAB, Dubey, R., Pessarkli, M., 2012. Reactive oxygen species, oxidative da mage, and antioxidativedefense mechanism in plants under stressful conditions. J. Bot. 2012, 1–26.
Sharma, S., Singh, V.K., Kumar, A., Mallubhotla, S., 2019. Effect of nanoparticles on oxidative damage and antioxidant defense system in plants. Mol. Plant Abiotic Stress Biol. Biotechnol. 315–333.
Shyam, R., Aery, N.C., 2012. Effect of cerium on growth, dry matter production, biochemical constituents and enzymatic activities of cowpea plants [Vignaun guiculata (L.) Walp.]. J. Soil Sci. Plant Nutr. 12 (1), 1–14.
Singh, A., Hussain, I., Singh, N.B., Singh, H., 2019. Uptake, translocation and impact of green synthesized nanoceria on growth and antioxidant enzymes activity of Solanum lycopersicum L. Ecotoxicol. Environ. Saf. 182, 109410.
Sinha, S., Saxena, R., Singh, S., 2005. Chromium induced lipid peroxidation in the plants of Pistia stratiotes L.: role of antioxidants and antioxidant enzymes. Chemosphere 85, 595–604.
Skiba, E., Pietrzak, M., Gapińska, M., Wolf, W.M., 2020. Metal homeostasis and gas exchange dynamics in Pisum sativum L. exposed to cerium oxide nanoparticles. Int. J. Mol. Sci. 21 (22), 8497.
Soliman, A.S., El-feky, S.A., Darwish, E., 2015. Alleviation of salt stress on Moringa peregrina using foliar application of nanofertilizers. J. Hortic. For. 7, 36–47.
Stewart, R.R.C., Bewley, J.D., 1980. Lipid peroxidation associated with accelerated aging of soybean axes. Plant Physiol. 65, 245–258.
Tang, W., Newton, R.J., 2005. Peroxidase and catalase activities are involved in direct adventitious shoot formation induced by thidiazuron in eastern white pine (Pinus strobes L.) zygotic embryos. Plant Physiol. Biochem. 43, 760–769.
Tanveer, K., Gilani, S., Hussain, Z., Ishaq, R., Adeel, M., Ilyas, N., 2020. Effect of salt stress on tomato plant and the role of calcium. J. Plant Nutr. 43 (1), 28–35.
Tombuloglu, H., Slimani, Y., Tombuloglu, G., Alshammari, T., Almessiere, M., Korkmaz, A.D., Samia, A.C.S., 2020. Engineered magnetic nanoparticles enhance chlorophyll content and growth of barley through the induction of photosystem genes. Environ. Sci. Pollut. Res. 27 (27), 34311–34321.
Tripathi, S.B., Gurumurthi, K., Panigrahi, A.K., Shaw, B.P., 2007. Salinity induced changes in proline and betaine contents and synthesis in two aquatic macrophytes differing in salt tolerance. Biol. Plant. 51 (1), 110–115.
Tumburu, L., Andersen, C.P., Rygiewicz, P.T., Reichman, J.R., 2017. Molecular and physiological responses to titanium dioxide and cerium oxide nanoparticles in Arabidopsis. Environ. Toxicol. Chem. 36 (1), 71–82.
Upadhyay, A., Gaonkar, T., Upadhyay, A.K., Jogaiah, S., Shinde, M.P., Kadoo, N.Y., Gupta, V.S., 2018. Global transcriptome analysis of grapevine (Vitis vinifera L.) leaves under salt stress reveals differential response at early and late stages of stress in table grape cv. Thompson Seedless. Plant Physiol. Biochem. 129, 168–179.
Walker, R.R., Blackmore, D.H., Clingeleffer, P.R., Correll, R.L., 2002. Rootstock effects on salt tolerance of irrigated field-grown grapevines (Vitis vinifera L. cv. Sultana).: 1. Yield and vigour inter-relationships. Aust. J. Grape Wine Res. 8, 3–14.
Wang, Q., Ma, X., Zhang, W., Pei, H., Chen, Y., 2012. The impact of cerium oxide nanoparticles on tomato (Solanum lycopersicum L.) and its implications for food safety. Metallomics 4, 1105–1112.
Wang, Y., Wang, L., Ma, C., Wang, K., Hao, Y., Chen, Q., Rui, Y., 2019. Effects of cerium oxide on rice seedlings as affected by co-exposure of cadmium and salt. Environ. Pollut. 252, 1087–1096.
Wang, Y., Zhang, P., Li, M., Guo, Z., Ullah, S., Rui, Y., Lynch, I., 2020. Alleviation of nitrogen stress in rice (Oryza sativa) by ceria nanoparticles. Environ. Sci. Nano 7 (10), 2930–2940.
Wu, D., Shen, Q., Cai, S., Chen, Z.H., Dai, F., Zhang, G., 2013. Ionomic responses and correlations between elements and metabolites under salt stress in wild and cultivated barley. Plant Cell Physiol. 54 (12), 1976–1988.
Wu, H., Tito, N., Giraldo, J.P., 2017. Anionic cerium oxide nanoparticles protect plant photosynthesis from abiotic stress by scavenging reactive oxygen species. ACS Nano 11 (11), 11283–11297.
Wu, H., Shabala, L., Shabala, S., Giraldo, J.P., 2018. Hydroxyl radical scavenging by cerium oxide nanoparticles improves Arabidopsis salinity tolerance by enhancing leaf mesophyll potassium retention. Environ. Sci. Nano 5 (7), 1567–1583.
Yildirim, E., Taylor, A.G., Spittler, T.D., 2006. Ameliorative effects of biological treatments on growth of squash plants under salt stress. Sci. Hortic. 111 (1), 1–6.
Yuanchun, M., Wang, J., Zhong, Y., Geng, F., Cramer, G.R., Cheng, Z.-M.M., 2015. Sub functionalization of cation/proton antiporter 1 genes in grapevine in response to salt stress in different organs. Hortic. Res. 2, 1–9.
Yuhui, M., Zhang, P., Zhang, Z., He, X., Li, Y., Zhang, J., Zheng, L., Chu, S., Yang, K., Zhao, Y., 2015. Origin of the different phytotoxicity and biotransformation of cerium and lanthanum oxide nanoparticles in cucumber. Nanotoxicology 9, 262–270.
Zayed, M.M., Elkafafi, S.H., Zedan, A.M., Dawoud, S.F., 2017. Effect of nano chitosan on growth, physiological and biochemical parameters of Phaseolus vulgaris under salt stress. J. Plant Prod. 8, 577–585.
Zhao, L., Peralta-Videa, J.R., Rico, C.M., Hernandez-Viezcas, J.A., Sun, Y., Niu, G., Servin, A., Nunez, J.E., Duarte-Gardea, M., Gardea-Torresdey, J.L., 2014. CeO2 and ZnO nanoparticles change the nutritional qualities of cucumber (Cucumis sativus). J. Agric. Food Chem. 62, 2752–2759.
Zheng, L., Hong, F., Lu, S., Liu, C., 2005. Effect of nano-TiO2 on strength of naturally aged seeds and growth of spinach. Biol. Trace Elem. Res. 104, 83–91.
Zulfiqar, F., Ashraf, M., 2021. Nanoparticles potentially mediate salt stress tolerance in plants. Plant Physiol. Biochem. 160, 257–268.